Intracellular performance of tailored nanoparticle tracers in magnetic particle imaging

Hamed Arami and Kannan M. Krishnan

Citation: Journal of Applied Physics **115**, 17B306 (2014); doi: 10.1063/1.4867756
View online: http://dx.doi.org/10.1063/1.4867756
View Table of Contents: http://scitation.aip.org/content/aip/journal/jap/115/17?ver=pdfcov
Published by the AIP Publishing

Intracellular performance of tailored nanoparticle tracers in magnetic particle imaging

Hamed Arami and Kannan M. Krishnan[a)]
Department of Materials Science and Engineering, University of Washington, P.O. Box 352120, Seattle, Washington 98195-2120, USA

(Presented 7 November 2013; received 12 September 2013; accepted 5 December 2013; published online 10 March 2014)

Magnetic Particle Imaging (MPI) is a quantitative mass-sensitive, tracer-based imaging technique, with potential applications in various cellular imaging applications. The spatial resolution of MPI, in the first approximation, improves by decreasing the full width at half maximum (FWHM) of the field-derivative of the magnetization, dm/dH of the nanoparticle (NP) tracers. The FWHM of dm/dH depends critically on NPs' size, size distribution, and their environment. However, there is limited information on the MPI performance of the NPs after their internalization into cells. In this work, 30 to 150 μg of the iron oxide NPs were incubated in a lysosome-like acidic buffer (0.2 ml, 20 mM citric acid, pH 4.7) and investigated by vibrating sample magnetometry, magnetic particle spectroscopy, transmission electron microscopy, and dynamic light scattering (DLS). The FWHM of the dm/dH curves of the NPs increased with incubation time and buffer to NPs ratio, consistent with a decrease in the median core size of the NPs from $\sim 20.1 \pm 0.98$ to $\sim 18.5 \pm 3.15$ nm. Further, these smaller degraded NPs formed aggregates that responded to the applied field by hysteretic reversal at higher field values and increased the FWHM. The rate of core size decrease and aggregation were inversely proportional to the concentration of the incubated NPs, due to their slower biodegradation kinetics. The results of this model experiment show that the MPI performance of the NPs in the acidic environments of the intracellular organelles (i.e., lysosomes and endosomes) can be highly dependent on their rate of internalization, residence time, and degradation. © *2014 AIP Publishing LLC*. [http://dx.doi.org/10.1063/1.4867756]

Magnetic particle imaging (MPI) is a non-invasive, tomographic biomedical imaging technique for visualizing distribution of superparamagnetic iron oxide nanoparticles (NPs) tracers in tissues, organs, and the vasculature.[1–3] The MPI signal is generated inductively only from the nanoparticle magnetization, and there is no interference from the surrounding diamagnetic tissues.[1,4] MPI also has a high mass sensitivity—down to 15 μg/ml—and the signal is linear with NPs concentration.[5] These promising characteristics make MPI a potentially useful technique for a wide range of clinical diagnostic and therapeutic applications, such as cardiovascular and cancer imaging, stem cell tracking, etc.

In MPI, an AC field with some amplitude, $\mu_0 H$, large enough to induce saturation in the non-linear magnetization response of NPs is applied. Due to the non-linear time-varying magnetization response of NPs, $M(t)$, a signal is induced in a detection coil. Further, this inductive signal can be localized by scanning a field-free point (FFP) or a field-free line (FFL) across the imaging volume.[2] In the *x-space* theory of MPI image reconstruction, the imaging efficiency (i.e., resolution and signal intensity) can be predicted by the point spread function (PSF) given as the product of magnetic field gradient ($G = dH/dx$, x: position) and the field-dependent derivative of the magnetization of the NPs, dm/dH. Here, G is a scanner-dependent parameter, and dm/dH is an intrinsic property of the NPs.[6–8] For a given MPI system, G is a constant, and the spatial resolution of the images generated can be improved by decreasing the full width at half maximum (FWHM) of the dm/dH.[5,9]

Superparamagnetic iron oxide NPs, being developed as MPI tracers,[10] are biodegredabale, biocompatible, and non-toxic and have been approved for various clinical applications by US food and drug administrative (FDA).[11,12] The monodispersity, core size, and environment-dependent relaxation mechanism of the iron oxide nanoparticles determine the signal intensity and spatial resolution of the MPI images.[5,13,14] Therefore, considering these parameters is crucial for successful utilization of MPI for *in vivo* imaging of carcinoma tissues or tracking of labeled cells in the future. However, the exact MPI performance of the NPs after cellular internalization is still unknown.

In this work, we studied the long-term MPI performance of monodisperse polyethylene glycol (PEG) coated NPs in a simulated lysosome solution.[15] Lysosomes are the main intracellular organelles, responsible for degradation of the NPs.[16] The results of our study show that depending on the concentration of the NPs, the degradation alters the size of the NPs and can cause their partial aggregation. These structural changes of the NPs in such intracellular environments increase the FWHM of their dm/dH curves, which eventually results in lowering the resolution of the MPI images. The degradation was inversely proportional to the concentrations of the NPs incubated in the lysosome-like solution, suggesting that higher cellular internalization might preserve the spatial resolution of MPI in future applications in cellular imaging.

Monodisperse hydrophobic iron oxide NPs were synthesized following a thermal decomposition method.[17,18] We used

[a)]Author to whom correspondence should be addressed. Electronic mail: kannanmk@uw.edu

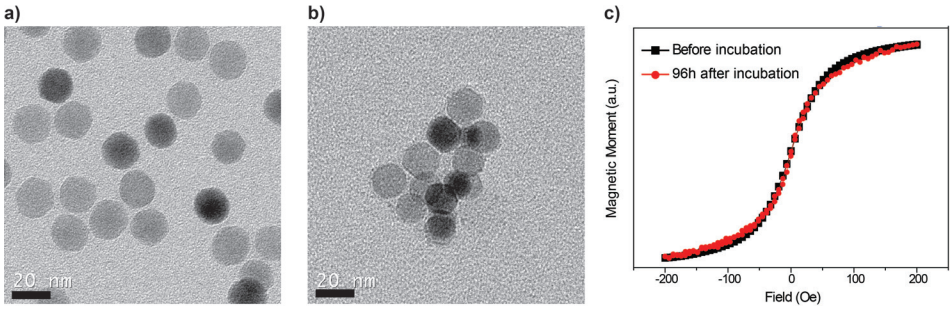

FIG. 1. TEM images of the PEG coated NPs before (a) and after (b) incubation (96 h) in lysosome-like (pH = 4.8) solution. Core sizes calculated by fitting the $m(H)$ plots of the NPs (c) to the Langevin function[19] confirmed the size variations observed in TEM images. Here, 30 μg of the NPs were incubated in 200 μl of the acidic solution.

a previously reported method to modify these NPs with PEG.[7] The size and morphology of the NPs were analyzed using transmission electron microscopy (TEM, FEI TecnaiTM G2 F20, 200 KeV, Hillsboro, OR), equipped with a Gatan CCD camera (Pleasanton, CA). A vibrating sample magnetometer (VSM, Lakeshore, Weterville, OH) was used to study the static magnetization behavior of the NPs (~150 μg of NPs in polycarbonate capsules) at room temperature. Assuming a log-normal size distribution, these magnetization, $m(H)$, curves were used to determine the median core size of the NPs.[19] Inductively Coupled Plasma Atomic Emission Spectrophotometer (ICP-AES, Jarrell Ash 955, US) was used to measure the iron concentrations in liquid samples. The hydrodynamic sizes of the NPs were determined using dynamic light scattering (Zetasizer Nano, Malvern Instruments, UK). A custom-built magnetic particle spectrometer (MPS) with a sinusoidal excitation field of 18.6 mT μ_0^{-1} (peak- peak, $f_0 = 25$ kHz) was used to investigate the MPI performance of the NPs followed by methods reported previously.[5,14,20]

To simulate the intracellular performance of the NPs, different amounts of the NPs (30, 50, 100, and 150 μg) were dispersed in 0.2 ml of 20 mM citric acid buffer with pH of 4.8.[15] The mixtures were then sealed and incubated at 37 °C for up to 96 h, and the MPS performances of the NPs were monitored over the incubation period. The size variations of the incubated NPs were also verified by TEM and VSM analyses as described above.

We used a ligand exchange method to replace the oleic acid molecules, capped on the surface of the monodisperse iron oxide NPs by TSP.[21] This process provides carboxyl groups onto the surface of the NPs.[22] Then, we conjugated amine-terminated PEG (NH_2-PEG-NH_2) to these carboxyl groups.[7] Dynamic light scattering measurements showed that the resulting hydrophilic NPs had a hydrodynamic size of about 82 nm. We have shown before that these NPs are highly stable in aqueous buffers (e.g., phosphate buffered solution or PBS) and biological media (e.g., cell culture media enriched with 10% fetal bovine serum) and show a consistent performance as efficient MPI tracers without notable change in their core and hydrodynamic sizes over a period of at least one week of incubation in these solutions.[7]

To simulate the MPI performance of these NPs after internalization into main cellular organelles (i.e., endosomes and lysosomes), we incubated 30 μg of the NPs in 0.2 ml of an acidic lysosome-like buffer solution[15] and determined their core and hydrodynamic size variations and MPS performance over a period of 4 days. TEM (Figs. 1(a) and 1(b)) and DLS (Fig. 3(b)) analysis showed that initially, monodisperse NPs were partially degraded after incubation and formed aggregates composed of these smaller size NPs. These aggregates can be potentially formed following detachment of the stabilizing PEG molecules from the surface of the degraded NPs. In agreement with the TEM observations, fitting of the VSM magnetization curves of these NPs to a Langevin function showed that their median core size decreased from ~20.1 ± 0.098 nm to ~18.5 ± 3.15 nm after incubation in acidic buffer for 96 h (Figs. 1(c) and 3(b)). As shown in Fig. 1(c), the slope, dm/dH, of the $m(H)$ curves of these smaller NPs was slightly less than the NPs prior to incubation. This degradation-dependent size decrease was slower when higher concentrations of the NPs (i.e., 50, 100, and 150 μg) were incubated in the same amount of the buffer solution (Fig. 3(b)). Also, the larger core size standard deviations after incubation (Fig. 3(b)) show that the degradation phenomenon increased the core size polydispersity of the NPs. Considering the same amount of the acidic solution for all the incubation conditions, the slower degradation of higher concentration of the NPs can be correlated to their larger total surface area exposed to the degrading solution.[15,23]

Spatial resolution of MPI images directly depends on the FWHM of the dm/dH curves of the NPs used as the contrast agent.[8] Using magnetic particles spectrometry, we have shown before that this FWHM parameter is highly dependent on the median core and hydrodynamic sizes and monodispersity of the NPs.[5,14,24] Therefore, partial dissolution and aggregation of the NPs in acidic buffer increases their FWHM (Figs. 2(a)–2(d) and 3(a)), which results in poor resolution in MPI images. This FWHM increase can be attributed to the resemblance of these aggregates to NPs with larger core sizes and their forced hysteretic reversal at higher magnetic field values (>5 mT).[5] Variation of the hydrodynamic sizes in Fig. 3(b) shows that at lower concentration of the NPs (e.g., 30 μg), higher percentage of these aggregates form during the incubation. These aggregates increase the average hydrodynamic size of the NPs and result in shifting the location of the MPS peak to higher field values (Fig. 2(a)) and formation of $m(H)$ curves with larger coercivity as shown in Fig. 2(e) for the applied field frequency ($f_0 = 25$kHz) used in our spectrometer. Similar to core size variation rates, this FWHM and coercivity increases were less for higher concentration of the incubated NPs (Figs. 2(a)–2(f) and 3(a)). The details of the relaxation mechanisms of the monodisperse NPs in the presence of the applied AC magnetic field (25 kHz) can be found in our previous reports.[5,7,9,13,25,26]

The future application of MPI for imaging of targeted tissues (such as cancers or atherosclerotic plaques) or

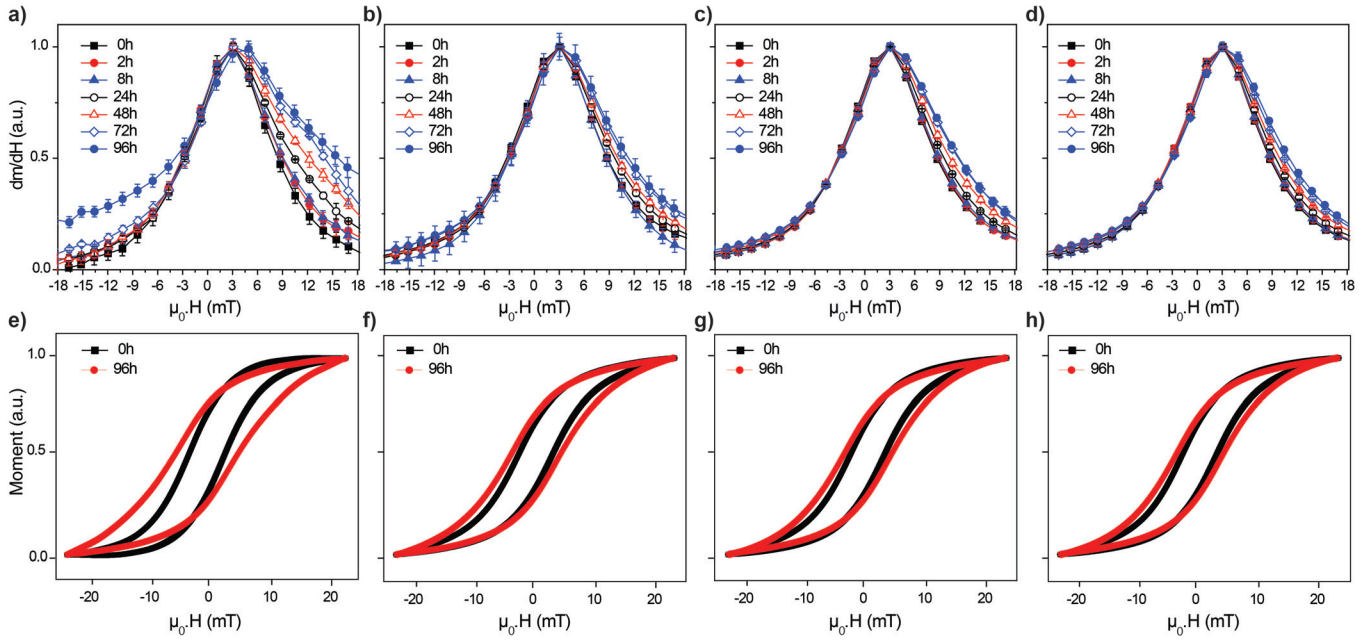

FIG. 2. The d*m*/d*H* plots ((a)–(d)), measured at 25 kHz in our Magnetic particle spectrometer,[13] were integrated to derive the corresponding *m*(*H*) curves ((e)–(h)). Different amounts of NPs—30 ((a) and (e)), 50 ((b) and (f)), 100 ((c) and (g)), and 150 μg ((d) and (h))—were incubated in lysosome-like buffer for 0–96 h.

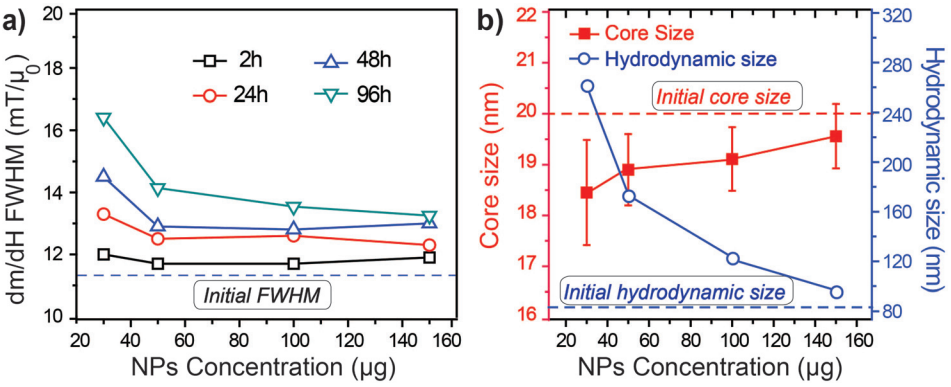

FIG. 3. (a) Change of the FWHM of d*m*/d*H* as a function of NPs concentration and incubation time at pH = 4.8. NPs' concentrations were held constant during each incubation experiment. Note that the lines connecting different concentrations of NPs for the same incubation times are intended as guides to the eye. (b) Core and hydrodynamic size variation by concentration of the NPs incubated for 96 h. The core sizes were calculated by fitting of the NPs *m*-*H* curves to the Langevin function, and the hydrodynamic sizes were determined using dynamic light scattering.

magnetically labeled cells (such as stem cells, macrophages, or red blood cells) depends on the consistent performance of the NPs after cellular internalization. Lysosomes, the most probable destination of the internalized NPs, are acidic (pH ~ 5.0) and this environment likely degrades the NPs in a short time. The spatial resolution in MPI is strongly correlated with the core size and polydispersity of the NPs. Therefore, this degradation phenomenon weakens the MPI performance of the NPs, and special surface modification strategies should be developed to tune the cellular internalization rate, pathways, and degradation rates of the NPs, based on the desired MPI application.

This work was supported by NIH Grant No. 1RO1EB013689-01/NIBIB. Part of this work was conducted at the University of Washington NanoTech User Facility, a member of the NSF National Nanotechnology Infrastructure Network (NNIN).

[1]J. Weizenecker *et al.*, Phys. Med. Biol. **54**, L1 (2009).
[2]B. Gleich and J. Weizenecker, Nature **435**, 1214 (2005).
[3]K. M. Krishnan, IEEE Trans. Magn. **46**, 2523 (2010).
[4]P. W. Goodwill *et al.*, Adv. Mater. **24**, 3870 (2012).
[5]H. Arami *et al.*, Med. Phys. **40**, 071904 (2013).
[6]A. P. Khandhar *et al.*, Biomaterials **34**, 3837 (2013).
[7]H. Arami and K. M. Krishnan, IEEE Trans. Magn. **49**, 3500 (2013).
[8]P. W. Goodwill and S. M. Conolly, IEEE Trans. Med. Imaging **29**, 1851 (2010).
[9]R. M. Ferguson *et al.*, "Magnetic Particle Imaging with Safe, Tailored Iron Oxide Nanoparticle Tracers," IEEE Trans. Med. Imaging (Submitted).
[10]M. H. Pablico-Lansigan *et al.*, Nanoscale **5**, 4040 (2013).
[11]A. B. Pai and A. O. Garba, J. Blood Med. **3**, 77 (2012).
[12]H. Arami *et al.*, Adv. Polym. Sci. **243**, 163 (2011).
[13]R. M. Ferguson *et al.*, Biomed. Eng. **58**, 493 (2013).
[14]R. M. Ferguson *et al.*, J. Appl. Phys. **111**, 07B318 (2012).
[15]L. Lartigue *et al.*, ACS Nano **7**, 3939 (2013).
[16]M. Levy *et al.*, Biomaterials **32**, 3988 (2011).
[17]S. Kalele *et al.*, J. Magn. Magn. Mater. **321**, 1377 (2009).
[18]R. Narain *et al.*, Langmuir **23**, 6299 (2007).
[19]R. Chantrell *et al.*, IEEE Trans. Magn. **14**, 975 (1978).
[20]I. Schmale *et al.*, in *Magnetic Particles Imaging*, edited by T. M. Buzug and J. Borgert (Springer, Germany, 2012), p. 279.
[21]M. Q. Zhu *et al.*, J. Mater. Chem. **17**, 800 (2007).
[22]C. Fang *et al.*, Small **5**, 1637 (2009).
[23]G. C. Baltazar *et al.*, PLOS One **7**, e49635 (2012).
[24]H. Arami *et al.*, in *Role of Biofunctionalization and Tracer Cross-Linking in Magnetic Particle Spectrometry*, (IEEE, Berkeley, US, 2013).
[25]R. M. Ferguson *et al.*, Med. Phys. **38**, 1619 (2011).
[26]R. M. Ferguson *et al.*, J. Magn. Magn. Mater. **321**, 1548 (2009).